Microchim Acta (2013) 180:1501–1507
DOI 10.1007/s00604-013-1032-5

ORIGINAL PAPER

A SERS-based immunoassay for porcine circovirus type 2 using multi-branched gold nanoparticles

Zhihui Luo · Wentao Li · Donglian Lu · Kun Chen · Qigai He · Heyou Han · Mingqiang Zou

Received: 1 February 2013 / Accepted: 10 June 2013 / Published online: 6 August 2013

Abstract We report on a facile immunoassay for porcine circovirus type 2 (PCV2) based on surface enhanced Raman scattering (SERS) using multi-branched gold nanoparticles (mb-AuNPs) as substrates. The mb-AuNPs in the immunosensor act as Raman reporters and were prepared via Tris base-induced reduction and subsequent reaction with p-mercaptobenzoic acid (pMBA). They possess good stability and high SERS activity. Subsequently, the modified mb-AuNPs were covalently conjugated to the monoclonal antibody (McAb) against the PCV2 cap protein to form SERS immuno nanoprobes. These were captured in a microtiterplate via a immunoreaction in the presence of target antigens. The effects of antibody concentration, reaction time and temperature on the sensitivity of the immunoassay were investigated. Under optimized assay conditions, the Raman signal intensity at 1,076 cm^{-1} increases logarithmically with the concentrations of PCV2 in the concentration ranging from 8×10^2 to 8×10^6 copies per mL. The limit of detection is 8×10^2 copies per mL. Compared to conventional detecting methods such as those based on PCR, the method presented here is rapid, facile and very sensitive.

Keywords Porcine circovirus type 2 · Immunoassay · Surface enhanced Raman scattering · Multi-branched gold nanoparticles

Z. Luo · D. Lu · K. Chen · H. Han (✉)
State Key Laboratory of Agricultural Microbiology, College of Science, Huazhong Agricultural University, Wuhan 430070, People's Republic of China
e-mail: hyhan@mail.hzau.edu.cn

W. Li · Q. He
College of Animal Science and Veterinary Medicine, State Key Laboratory of Agricultural Microbiology, Huazhong Agricultural University, Wuhan 430070, People's Republic of China

M. Zou (✉)
Chinese Academy of Inspection and Quarantine, Beijing 100025, People's Republic of China
e-mail: mingqiangz@sina.com

Introduction

The development of rapid and highly sensitive methods for pathogen detection is central to human health, veterinary medicine, and biodefense [1]. Animal diseases can not only cause huge economic loss, but also endanger human health. Porcine circovirus (PCV) is a non-enveloped, circular, single-stranded DNA virus with genome of about 1.76 kb and a size of 17 nm in diameter [2, 3]. PCV have two species, one is PCV1, considered to be nonpathogenic to swine; the other is PCV2, an important source of severe swine diseases, including the postweaning multisystemic wasting syndrome (PMWS), porcine respiratory disease complex (PRDC) and porcine dermatitis and nephropathy syndrome (PDNS) [4–6], which caused great losses to the swine industry. The infectious diseases with PCV2 were mostly characterized by a steady loss of weigh, feverish, respiratory difficulty and jaundice. In 1996, the outbreak of PMWS caused by PCV2 was first reported in Canada, and was found in several other countries since then [7]. Based on it, at the 20th International Pig Veterinary Society Congress in 2008, PCV-associated disease was listed as the first disease which threatens the development of the swine industry. At present, several protocols have been applied to detect PCV2 including polymerase chain reaction (PCR), enzyme-linked immunosorbent assay and indirect immunofluorescence assay [8–11]. The detecting methods mentioned above play a certain role in PCV2 diagnosis, yet they are susceptible to interference, lower sensitivity, operation cumbersome and prone to false-positive reaction. Thus, it is vital to develop a simple, rapid and sensitive detecting method for PCV2 to diagnose and handle the diseases.

Surface-enhanced Raman scattering (SERS) is a rapid, nondestructive and highly sensitive analytical technique, which has been widely applied in biological analysis and imaging, molecular and nanoparticle characterization as well as multiplex high-throughput detection [12–15]. SERS substrates such as spherical, rod like and multi-branched noble

metal nanoparticles, has attracted particular attention due to their unique structure and optical properties [16]. Among these SERS substrates, multi-branched gold nanoparticles (mb-AuNPs) are one of most attractive SERS substrates because their plasmon absorption band locates in the near-infrared to red spectral region which causes minimal interference from the biological specimen autofluorescence upon red laser excitation. Additionally, mb-AuNPs exhibit high SERS enhancement factors due to their sharp tips and gaps [17, 18].

Until now, great efforts have been made toward the innovative synthetic techniques of mb-AuNPs such as surfactant directing method [19, 20], electrochemical method [21], hydrothermal method [22], vapor phase polymerization method [23] and seedless in situ growth method [24, 25]. However, rational design of the SERS immunoassay based on mb-AuNPs remains little explored due to the difficulty of modification and the intrinsically cytotoxicity of surfactant. Recently, we reported a facile method for preparing high-quality mb-AuNPs using tris base (TB) as the ideal reducing agent without any surfactant or seed. As a SERS-active substrate, the mb-AuNPs performed good biocompatibility and high SERS activity and have been successfully applied in cell imaging [26].

Herein, a simple, rapid and sensitive SERS immunoassay employing mb-AuNPs as substrates has been developed for the determination of PCV2. Scheme 1 describes the fabrication process of the SERS-based immunosensor. PCV2 was first anchored onto the microtiterplate (MTP). The Raman reporter p-mercaptobenzoic acid (pMBA) tagged mb-AuNPs were covalently linked to PCV2 McAb through a 1-ethyl-3-(3-dimethylaminopropyl) carbodiimide (EDC) coupling process. Then the SERS nanoprobe was captured on the plate via a immunoreaction. Due to the increasing number of captured nanoprobes, the SERS signal from pMBA was greatly enhanced which favored the sensitive detection of PCV2. The results suggested that the method possessed excellent potential for diagnostic immunoassay.

Experimental

Chemicals and materials

Hydrochloroauric acid trihydrate, tris base were purchased from Sinopharm Chemical Reagent Co., p-mercaptobenzoic acid (pMBA) was obtained from Tokyo Chemical Industry Co., Ltd. (http://www.tci-asiapacific.com). 1-ethyl-3-[3-(dimethylamino)propyl] carbodiimide (EDC) and N-hydroxysuccinimide (NHS) were obtained from Sigma (http://www.sigmaaldrich.com/china-mainland.html). Goat anti-mouse IgG-FITC were obtained from southernbiotech,USA (http://www.amyjet.com/news/sba-china-distributor.shtml). PCV2, PCV2 cap protein monoclonal antibody (McAb), porcine parvovirus (PPV), porcine reproductive and respiratory syndrome virus (PRRSV), porcine pseudorabies virus (PRV) and serum samples of infected pigs were provided by State Key Laboratory of Agricultural Microbiology, Huazhong Agricultural University, China. The buffers used were as follows: (A) 10 mM sodium phosphate buffered saline (PBS), pH 7.2; (B) washing solution, buffer A with 0.1 % Tween, Other chemicals were all of reagent grade and used without further purification. Ultrapure deionized water was used throughout the experiments.

Instrumentation

SERS measurements were performed using inVia Raman spectrometer (Renishaw, UK, http://www.renishaw.com) equipped with a focusing microscope (Leica, German, http://www.leica-microsystems.com). A He-Ne laser (633 nm) was used as the excitation source with a laser power of approximately 1.7 mW on the sample. Calibration was done referring to the 520 cm^{-1} line of silicon. The SERS spectra were obtained with the exposure time of 10 s and one time accumulation. The UV–vis absorption spectra were recorded on Thermo Nicolet 300 spectro-

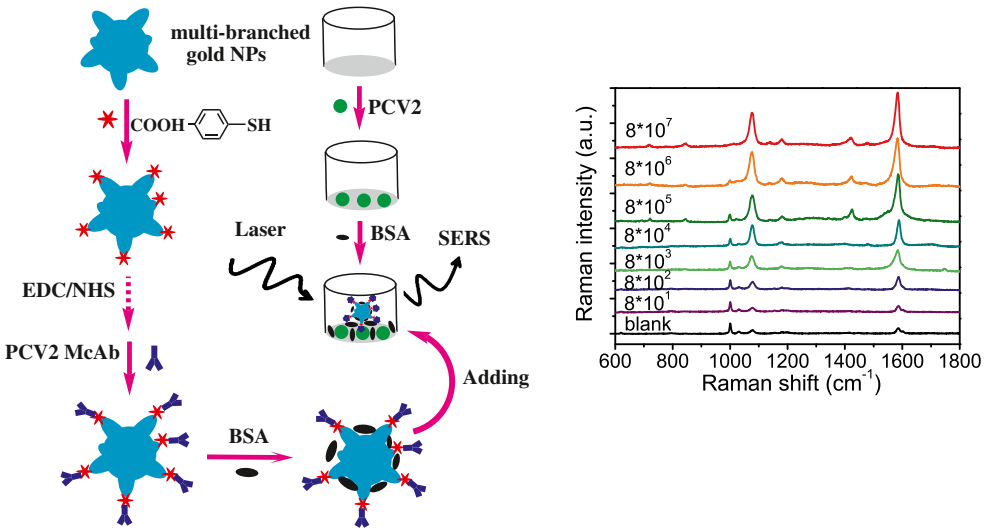

Scheme 1 Schematic representation of the determination procedure for PCV2 using MPPM

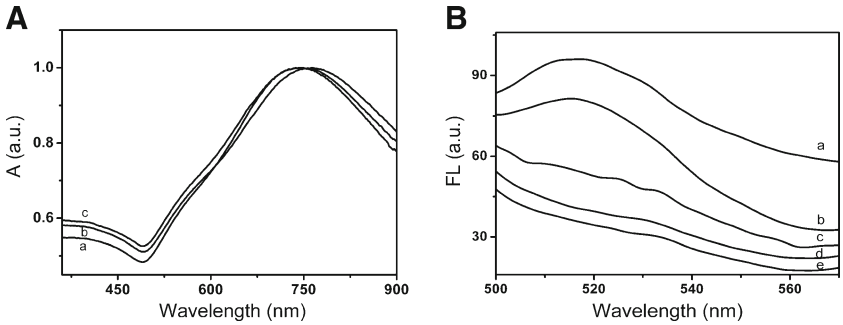

Fig. 1 (**A**) The UV–vis absorption spectra of the mb-AuNPs (**a**), mb-AuNPs-pMBA (**c**) and MPPM (**b**). (**B**) FL spectra of goat anti-mouse IgG-FITC (**a**), goat anti-mouse IgG-FITC-MPPM (**b**), MPPM (**b**), mb-AuNPs-pMBA (**d**), and mb-AuNPs(**e**)

photometer (Thermo Nicolet, the United Stated, http://www.thermoscientific.com). The fluorescence spectra were performed on a Perkin Elmer Model LS-55 luminescence spectrometer (Perkin Elmer, the United Stated, http://www.perkinelmer.com). The morphologies of mb-AuNPs were obtained from transmission electron microscope (TEM, Hitachi-7650, Japan, http://www.hitachi-hitec.com).

Synthesis of mb-AuNPs

Mb-AuNPs were prepared in a one-step process according to our early work [26]. In a typical synthesis, 0.27 g TB was dissolved in 5 mL of ultrapure water, and 100 μL of 48-mmol L^{-1} $HAuCl_4$ solution was added under magnetic stirring for 15 min, followed by adjusting the pH to 10–11 by dropwise addition of 1.0 mol L^{-1} NaOH solution. Afterward, the reaction vessel was transferred to water bath and maintained at 60 °C for 60 min. The solution color changed from light yellow to purple and finally blue-green. The products were purified for three times by centrifugation at 6,000 rpm and the resultant precipitates were re-dissolved in ultrapure water for further use.

Preparation of mb-AuNPs-pMBA-PCV2 McAb (MPPM)

40 μL of 1×10^{-3} mol L^{-1} pMBA was slowly added to 4 mL purified mb-AuNPs solution, and the 4-MBA molecules were covalently linked to the surface of mb-AuNPs through the S-Au bond under gently stirring. After reaction for 60 min at room temperature, the solution was centrifuged at 6,000 rpm for 8 min, and the supernatant containing uncombined pMBA was discarded. The precipitates were resuspended in 4 mL of 10 mM PBS. For the activation of carboxy groups of MBA, 10 μL of 5 mmol L^{-1} EDC and 10 μL of 5 mmol L^{-1} NHS were added and allowed to react for 1 h [27, 28]. In order to remove unreacted EDC/NHS, the solution was washed twice with PBS by centrifugation at 6,000 rpm for 8 min. 200 μL of 2.6 mg mL^{-1} PCV2 McAb were added to above active mb-AuNPs solution at 37 °C humidity chamber. After reacted for 60 min, the conjugated products was centrifuged at 6,000 rpm for 8 min, and then the sediment was resuspended with 1 % BSA in PBS for 2 h at room temperature, the MPPM were obtained after centrifuged and stored at 4 °C.

Preparation of serum samples

The preparation procedure of serum samples were as followed. Venous blood was took from infected and non-infected pigs and stored at 37 °C for 60 min, and then the blood was centrifuged at 5,000 rpm for 10 min, The resultant human serum sample was then stored at −70 °C until used.

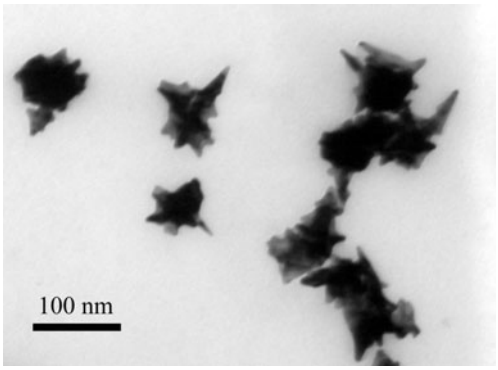

Fig. 2 TEM image of the obtained mb-AuNPs

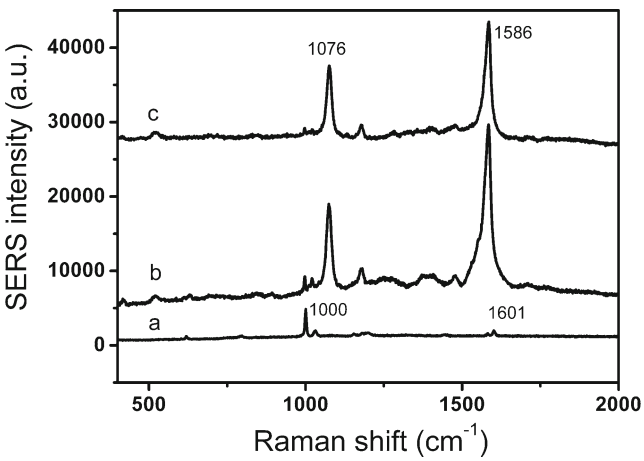

Fig. 3 SERS of MTP (**a**), mb-AuNPs-pMBA (**b**) and MPPM (**c**)

Immunoassay protocol

Immunoassay protocol was carried out according to the developed procedures with slight modifications [29]. Typically, the PCV2 (8×10^7 copies mL^{-1}) was dropped to the MTP with 100 μL per well, and incubated for 12 h at 4 °C. And then, the MTP was washed three times with washing buffer. After that, the residual sites of each well was blocked with 50 μL 3 % BSA in PBS and incubated for 60 min at 37 °C, the wells were washed with washing solution six times. At last, 100 μL MPPM were pipetted onto each well, after incubating at 37 °C for 60 min, each well of the plate was washed six times with washing solution. SERS detection was carried out after dried with nitrogen.

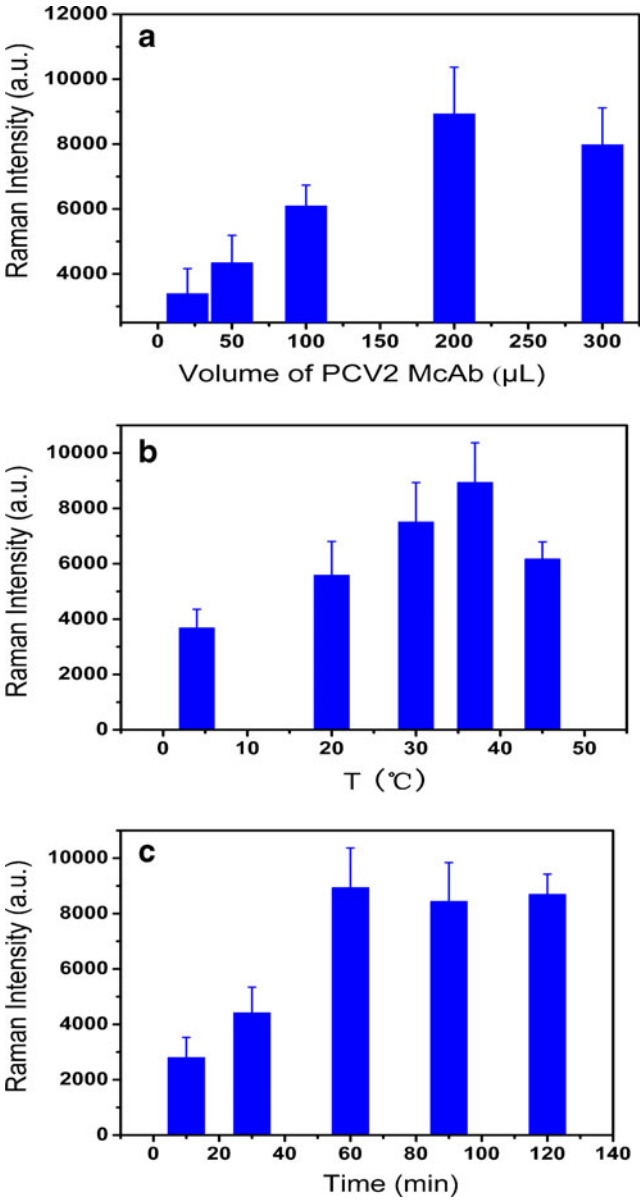

Fig. 4 The SERS intensity of nanoprobes at 1,076 cm^{-1} in response to different of PCV2 McAb concentration (**a**), temperature (**b**) and immunoreaction time (**b**). *Error bars* indicate standard deviations from five measurements

Results and discussion

Characterization of mb-AuNPs and MPPM

As shown in Fig. 1A, the UV–vis absorption spectra of the synthesized mb-AuNPs shows a maximum surface plasmon absorbance peak at 742 nm (Fig. 1Aa), and the result was consistent with the absorption features of mb-AuNPs prepared by previously reported methods [16, 24, 30]. The MPPM were prepared though a two-step process. First, pMBA, a common Raman reporter, was added to mb-AuNPs solution which caused the surface plasmon band of mb-AuNPs shifted from 742 to 744 nm (Fig. 1Ac) and full width at half maximum broadened from 170 to 185 nm. These results indicated pMBA molecules were covalently linked on the surfaced of mb-AuNPs by strong S-Au bonding interaction. When PCV2 McAb was added to the NHS activated mb-AuNPs, the plasmon resonance peak of MPPM altered to 760 nm (Fig. 1Ab). This indicated PCV2 McAb was conjugated to mb-AuNPs-MBA [31]. In order to prove the SERS probes (MPPM) were connected with the monoclonal antibody (McAb) of PVC2, fluorescent labeling was employed to monitor the reaction products using the FITC labeled second antibody. Fluorescence labeling experiment was employed to characterize the reaction products using the FITC labeled second antibody as readout signal. As shown in Fig. 1B, goat anti-mouse IgG-FITC-MPPM had an obvious emission peak at 515 nm (Fig. 1Ba) under excitation while no emission peaks were observed with the MPPM without incubation, mb-AuNPs-pMBA and mb-AuNPs with incubation. The obtained results successfully indicated that the monoclonal antibody (McAb) has linked to the MPPM, and the result was in accordance with that of UV–vis. The

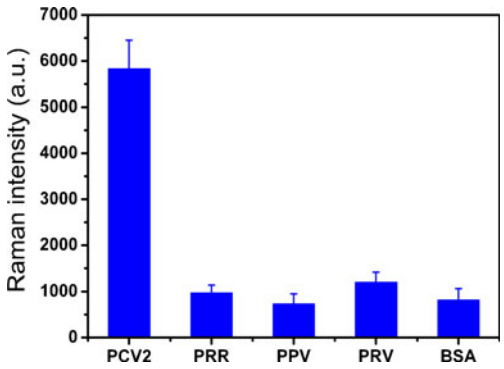

Fig. 5 The SERS intensity of nanoprobes at 1,076 cm^{-1} in respose to PCV2, PRR, PPV PRV and BSA. Experimental conditions: temperature 37 °C; and immunoreaction time 60 min. *Error bars* indicate standard deviations from five measurements

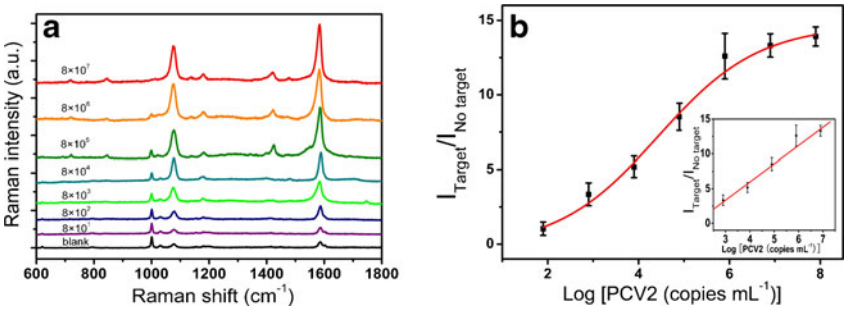

Fig. 6 (**a**) SERS spectra for decreasing concentrations of PCV2. Experimental conditions: temperature 37 °C; and immunoreaction time 60 min. (**b**) plot ratios of SERS intensities with and without the sample versus a series concentration of PCV2. Insert: the linear relationship of $I_{Target}/I_{No\ target}$ versus PCV2 concentration from 8×10^2 to 8×10^6 copies mL^{-1}. *Error bars* indicate standard deviations from five measurements

morphologies of mb-AuNPs were characterized by TEM, as depicted in Fig. 2. It is clear that mb-AuNPs have many branches on the rough surface, which may provide considerable 'hot spots' due to localized electromagnetic field enhancement.

Response performances in SERS

SERS performances of mb-AuNPs-pMBA, MPPM and MTP were tested respectively. It was known that optical hot spots of mb-AuNPs were frequently formed at the junctions or gaps [24, 32, 33]. As shown in Fig. 3, the SERS signal of mb-AuNPs-pMBA, MPPM were observed from 400 cm^{-1} to 2,000 cm^{-1}. The prominent SERS bands at 1,076 and 1,586 cm^{-1} are ascribed to the ν_{12} and ν_{8a} aromatic ring vibrations, respectively [34, 35]. Comparing the intensity of curve b with curve c at 1,076 and 1,586 cm^{-1} in Fig. 3, we found that their intensities changed little, indicating the PCV2 McAb conjugated nanoprobes remained a good SERS activity. We also investigated the interference of Raman spectra of the MTP. As shown in Fig. 3 (curve a), the Raman signals of MTP were obtained at 1,000 and 1,600 cm^{-1} in the absence of mb-AuNPs-pMBA or MPPM. It was clear that the peak at 1,076 cm^{-1} which was used to quantify PCV2 was not disturbed by the peaks of MTP at 1,000 and 1,600 cm^{-1}.

Optimization of immunoassay conditions

In the experiment, the amount of PCV2 McAb on the surface of mb-AuNPs played a critical role in SERS response. As shown in Fig. 4a, with the increase of PCV2 McAb concentration, the signal of MPPM gradually increased and reached a max platform, possibly due to the improved recognization in the immunoreaction. Thus, 200 μL of 2.6 mg mL^{-1} PCV2 McAb was chosen throughout the immunoassay.

The effects of immunoreaction temperature and immunoreaction time on the sensitivity of the immunoassay were investigated. As depicted in Fig. 4b, the SERS intensity of mb-AuNPs was dependent on the immunoreaction temperature. As the temperature increased from 4 °C to 37 °C, the SERS intensity gradually increased and reached a maximum at 37 °C. However, when immunoreaction temperature increased to 45 °C, the SERS intensity of mb-AuNPs was decreased. This may be attributed to the formation of unstable immunocomplexes or deterioration of proteins at higher temperature. The effect of time on the SERS response is shown in Fig. 4c. With the increase of reaction time from 10 to 60 min, the SERS intensity of mb-AuNPs gradually increased and reached a plateau at 60~90 min. To improve the sensitivity and efficiency, 37 °C and 60 min were selected as optimum immunoassay temperature and time, respectively, throughout subsequent testing.

Nonspecific experiment

In order to investigate the selectivity of MPPM towards PCV2, control experiments were carried out using other swine virus, including PRR, PPV and PRV. As shown in Fig. 5, an obvious high intensity of SERS signal at 1,076 cm^{-1} could be obtained in response to PCV2 (8×10^4 copies mL^{-1}), while the SERS signal of PRR, PPV, PRV at high concentration (1×10^5 copies mL^{-1}) were significantly lower than PCV2. So did the blocking protein (BSA). The results revealed that the MPPM were selective and specific towards PCV2.

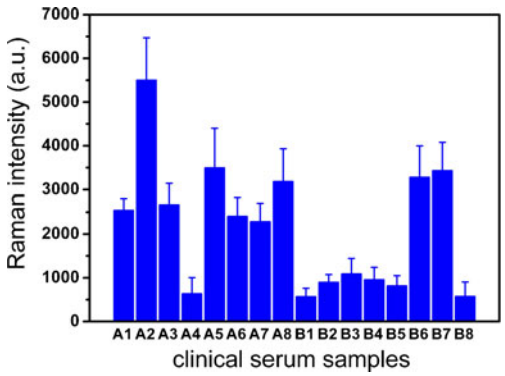

Fig. 7 Clinical serum samples analysis by SERS assay. *Error bars* indicated standard deviations from five measurements. Experimental conditions: temperature 37 °C; and immunoreaction time 60 min

SERS detection for PCV2

To improve the sensitivity and efficiency, 200 μL of 2.6 mg-mL^{-1} PCV2 McAb, 37 °C and 60 min were selected as optimum immunoassay condition to obtain the calibration graph in our experiment. The analytical performance was assessed by measuring the SERS intensity at 1,076 cm^{-1} response to the concentration of PCV2. Figure 6a shows the SERS spectra for a series concentration of PCV2. In the absence of PCV2, a weak SERS signal was obtained (blank), indicating that a small amount of MPPM still remained on the MTP after washing. when the concentration of PCV2 was added, the SERS intensity at 1,076 cm^{-1} were obviously enhanced with the concentration of PCV2 from 8×10^2 to 8×10^7 copies mL^{-1}. Here, the limit of detection was estimated to be 8×10^2 copies mL^{-1} according to the 3σ rule (where σ is the standard deviation of a blank), indicating a high sensitivity for virvus detection. Compared with the PCR methods (LOD: 1×10^5 copies mL^{-1}) [8], the LOD of this assay was two orders of magnitude lower. To efficiently mitigate the effect of instrumental complications, $I_{Target}/I_{No\ target}$ (the target/blank intensity ratio) was used as the measure to obtain the calibration graph, where were the intensities at 1,076 cm^{-1}in response to some concentration of PCV2 and PBS under the same conditions, respectively. As shown in Fig. 6b, a linear regression equation (y=2.62x-4.52 (R=0.99)) was obtained between the logarithm of PCV2 concentration (8×10^2~8×10^6 copies mL^{-1}) and the SERS intensity at 1,076 cm^{-1}. Compared with our previously reported chemiluminescence immunoassay [29], the SERS method is rapid and simple without dissolving the metal nanoparticles, while the sensitivity was in the same level.

To evaluate the application performance of the method, 16 clinical serum samples were analyzed. Comparing to the SERS intensity of blank control spectra at 1,076 cm^{-1}, the SERS detection results are shown in Fig. 7. For the detection of 8 positive serum by PCR, 7 serum was detected as positive by SERS method (A1−A8), the positive accordance rate of SERS detection to PCR were 87.5 %; For 8 negative serum by PCR, 6 serum was detected as negative by SERS method (B1–B8), the negative accordance rate of SERS detection to PCR were 75 %. This indicates the current method is in good accordance with PCR for the detection of PCV2. As a result, this method provides remarkable advantages in rapid, high sensitive and specific detection of animal disease.

Conclusions

In summary, we took advantage of mb-AuNPs to develop a novel biosensor for the detection of PCV2. The synthesis of mb-AuNPs was simple, rapid, inexpensive, and the fabricated probe possessed high SERS activity and high sensitivity. Under optimized assay conditions, the method was used to detect PCV2 over a wide concentration range (8×10^2~8×10^6 copies mL^{-1}) and with a low detection limit (8×10^2 copies mL^{-1}). Furthermore, this method was applied to detect 16 clinical serum, and the results suggested that SERS method had high positive (87.5 %) and negative (75 %) accordance rate with traditional method (PCR). As a result, the SERS strategy offered simple operation, good specificity and high sensitivity for virus detection and shows great potential in diagnosing, controlling and preventing animal-borne disease outbreaks.

Acknowledgments The authors gratefully acknowledge the financial support for this research from National Natural Science Foundation of China (21175051), the Fundamental Research Funds for the Central Universities (2010PY009, 2010PY139) and the natural science foundation of Hubei province innovation team (2011CDA115).

References

1. Chomel BB (2003) Control and prevention of emerging zoonoses. J Vet Med Edu 30:145–147
2. Allan GM, Ellis JA (2000) Porcine circoviruses: a review. J Vet Diagn Invest 12:3–14
3. Tischer I, Gelderblom H, Vettermann W, Koch M (1982) A very small porcine virus with circular single-stranded DNA. Nature 295:64–66
4. Chae C (2005) A review of porcine circovirus 2-associated syndromes and diseases. Vet J 169:326–336
5. Ellis J, Krakowka S, Lairmore M, Haines D, Bratanich A, Clark E, Allan G, Konoby C, Hassard L, Meehan B, Martin K, Harding J, Kennedy S, McNeilly F (1999) Reproduction of lesions of postweaning multisystemic wasting syndrome in gnotobiotic piglets. J Vet Diagn Invest 11:3–14
6. Choi J, Stevenson GW, Kiupel M, Harrach B, Anothayanontha L, Kanitz CL, Mittal SK (2002) Sequence analysis of old and new strains of porcine circovirus associated with congenital tremors in pigs and their comparison with strains involved with postweaning multisystemic wasting syndrome. Can J Vet Res 66:217–224
7. Harding J (1996) Postweaning multisystemic wasting syndrome: preliminary epidemiology and clinical findings. In 1996. In: Proc Western Can Assoc Swine Pract. p 21
8. Chang GN, Hwang JF, Chen JT, Tsen HY, Wang JJ (2010) Fast diagnosis and quantification for porcine circovirus type 2 (PCV-2) using real-time polymerase chain reaction. J Microbiol Immunol 43:85–92
9. Nawagitgul P, Harms PA, Morozov I, Thacker BJ, Sorden SD, Lekcharoensuk C, Paul PS (2002) Modified indirect porcine circovirus (PCV) type 2-based and recombinant capsid protein (ORF2)- based enzyme-linked immunosorbent assays for detection of antibodies to PCV. Clin Vaccine Immunol 9:33
10. Walker IW, Konoby CA, Jewhurst VA, McNair I, McNeilly F, Meehan BM, Cottrell TS, Ellis JA, Allan GM (2000) Development and application of a competitive enzyme-linked immunosorbent assay for the detection of serum antibodies to porcine circovirus type 2. J Vet Diagn Invest 12:400–405
11. Racine S, Kheyar A, Gagnon CA, Charbonneau B, Dea S (2004) Eucaryotic expression of the nucleocapsid protein gene of porcine circovirus type 2 and use of the protein in an indirect

immunofluorescence assay for serological diagnosis of postweaning multisystemic wasting syndrome in pigs. Clin Diagn Lab Immunol 11:736–741
12. Hu J, Zhao B, Xu W, Li B, Fan Y (2002) Surface-enhanced Raman spectroscopy study on the structure changes of 4-mercaptopyridine adsorbed on silver substrates and silver colloids. Spectroch Acta Part A 58:2827–2834
13. Guo X, Guo Z, Jin Y, Liu Z, Zhang W, Huang D (2012) Silver–gold core-shell nanoparticles containing methylene blue as SERS labels for probing and imaging of live cells. Microchim Acta 178:229–236
14. Shao M, Lu L, Wang H, Luo S, Ma D (2009) Microfabrication of a new sensor based on silver and silicon nanomaterials, and its application to the enrichment and detection of bovine serum albumin via surface-enhanced Raman scattering. Microchim Acta 164:157–160
15. Alvarez-Puebla RA, Liz-Marzán LM (2012) Traps and cages for universal SERS detection. Chem Soc Rev 41:43–51
16. Xie J, Zhang Q, Lee JY, Wang DIC (2008) The synthesis of SERS-active gold nanoflower tags for in vivo applications. ACS Nano 2:2473–2480
17. Schutz M, Steinigeweg D, Salehi M, Kompe K, Schlucker S (2011) Hydrophilically stabilized gold nanostars as SERS labels for tissue imaging of the tumor suppressor p63 by immuno-SERS microscopy. Chem Commun 47:4216–4218
18. Esenturk EN, Walker ARH (2009) Surface-enhanced Raman scattering spectroscopy via gold nanostars. J Raman Spectrosc 40:86–91
19. Sau TK, Murphy CJ (2004) Room temperature, high-yield synthesis of multiple shapes of gold nanoparticles in aqueous solution. J Am Chem Soc 126:8648–8649
20. Nehl CL, Liao H, Hafner JH (2006) Optical properties of star-shaped gold nanoparticles. Nano Letters 6:683–688
21. Xu X, Jia J, Yang X, Dong S (2010) A templateless, surfactantless, simple electrochemical route to a dendritic gold nanostructure and its application to oxygen reduction. Langmuir 26:7627–7631
22. Tang XL, Jiang P, Ge GL, Tsuji M, Xie S-S, Guo YJ (2008) Poly(N-vinyl-2-pyrrolidone) (PVP)-capped dendritic gold nanoparticles by a one-step hydrothermal route and their high SERS effect. Langmuir 24:1763–1768
23. Tamil Selvan S (1998) Novel nanostructures of gold-polypyrrole composites. Chem Commun 3:351–352
24. Bakr OM, Wunsch BH, Stellacci F (2006) High-yield synthesis of multi-branched urchin-like gold nanoparticles. Chem Mater 18:3297–3301
25. Jeong G, Lee Y, Kim M, Han S (2009) High-yield synthesis of multi-branched gold nanoparticles and their surface-enhanced Raman scattering properties. J Colloid Interf Sci 329:97–102
26. Luo Z, Fu T, Chen K, Han H, Zou M (2011) Synthesis of multi-branched gold nanoparticles by reduction of tetrachloroauric acid with Tris base, and their application to SERS and cellular imaging. Microchim Acta 175:55–61
27. Chon H, Lee S, Son SW, Oh CH, Choo J (2009) Highly sensitive immunoassay of lung cancer marker carcinoembryonic antigen using surface-enhanced Raman scattering of hollow gold nanospheres. Anal Chem 81:3029–3034
28. Park JH, Park J, Dembereldorj U, Cho K, Lee K, Yang SI, Lee SY, Joo SW (2011) Raman detection of localized transferrin-coated gold nanoparticles inside a single cell. Anal Bioanal Chem 401:1635–1643
29. Zhang H, Li W, Sheng Z, Han H, He Q (2010) Ultrasensitive detection of porcine circovirus type 2 using gold (III) enhanced chemiluminescence immunoassay. Analyst 135:1680–1685
30. Wang Z, Zhang J, Ekman JM, Kenis PJA, Lu Y (2010) DNA-mediated control of metal nanoparticle shape: one-Pot synthesis and cellular uptake of highly stable and functional gold nanoflowers. Nano Letters 10:1886–1891
31. Basu S, Ghosh SK, Kundu S, Panigrahi S, Praharaj S, Pande S, Jana S, Pal T (2007) Biomolecule induced nanoparticle aggregation: effect of particle size on interparticle coupling. J Colloid Interface Sci 313(2):724–734
32. Giannini V, Rodríguez-Oliveros R, Sánchez-Gil J (2010) Surface Plasmon resonances of metallic nanostars/nanoflowers for surface-enhanced Raman scattering. Plasmonics 5:99–104
33. Wang H, Halas N (2008) Mesoscopic Au "meatball" particles. Adv Mater 20:820–825
34. Michota A, Bukowska J (2003) Surface-enhanced Raman scattering (SERS) of 4-mercaptobenzoic acid on silver and gold substrates. J Raman Spectrosc 34:21–25
35. Orendorff CJ, Gole A, Sau TK, Murphy CJ (2005) Surface-enhanced Raman spectroscopy of self-assembled monolayers: sandwich architecture and nanoparticle shape dependence. Anal Chem 77:3261–3266